International Journal of Applied Pharmaceutics

ISSN- 0975-7058 Vol 17, Issue 1, 2025

Original Article

ULTRA-FAST SYNTHESIS OF CURCUMIN-LOADED SILVER NANOPARTICLES: IMPROVED PHYSICOCHEMICAL PROPERTIES FOR DRUG DELIVERY

CHONG XUE LI[1], GAMAL OSMAN ELHASSAN[2], SIHAM A. ABDOUN[2], RIYAZ AHMED KHAN[2], MANOJ GOYAL[3], MONIKA BANSAL[4], JAMAL MOIDEEN MUTHU MOHAMED[1]*

[1]Faculty of Pharmacy and BioMedical Sciences, MAHSA University, Bandar Saujana Putra, 42610 Jenjarom, Selangor, Malaysia. [2]Department of Pharmaceutics, College of Pharmacy, Qassim University, Buriadah, K. S. A. [3]Department of Anesthesia Technology, College of Applied Medical Sciences in Jubail, Imam Abdul Rahman Bin Faisal University, Dammam, Saudi Arabia. [4]Department of Neuroscience Technology, College of Applied Medical Sciences in Jubail, Imam Abdul Rahman Bin Faisal University, Dammam, Saudi Arabia
*Corresponding author: Jamal Moideen Muthu Mohamed; *Email: jamalmoideen@mahsa.edu.my

Received: 13 Sep 2024, Revised and Accepted: 16 Nov 2024

ABSTRACT

Objective: This study focused on the green synthesis of silver nanoparticles (AgNPs) using fresh garlic extract (*Allium sativum*-AS) as a reducing agent for the efficient delivery of curcumin (CuR), a natural anti-cancer agent used in breast cancer therapy.

Methods: The study began with the preparation of fresh AS, which was then mixed with silver nitrate ($AgNO_3$) solution and CuR solution under sunlight for the green synthesis of stable CuR-loaded nanoparticles (C-AgNPs). This method not only offered an eco-friendly approach to the synthesis of C-AgNPs but also highlighted the potential physicochemical characterization of AS and CuR in this context. Moreover, this study assesses the characteristics of the resulting C-AgNPs and conducts a comparative analysis with different formulations to evaluate their efficacy.

Results: The prepared C-AgNPs, characterized by Fourier-Transform Infrared Spectroscopy (FTIR), indicated that CuR, silver nitrate ($AgNO_3$), and AS extract were successfully incorporated, confirming the successful synthesis. The optimized preparation, referred to as AgNP1, demonstrated an entrapment efficacy of 74.24±5.87%, a drug loading of 95.99±7.81%, and a drug content of 96.11±7.82%. Additionally, the cumulative percentage of drug release was found to be 57.12±2.76% at 180 min. The drug was successfully loaded into the C-AgNPs, exhibiting physicochemical compatibility without any adverse chemical interactions with the additives used.

Conclusion: In conclusion, this study demonstrated that nanoparticle-based drug delivery systems offer a significant advancement over conventional therapies by providing controlled and efficient drug delivery, thereby improving therapeutic outcomes.

Keywords: Drug delivery, Green synthesis, Drug formulation, AgNPs, Curcumin, *In vitro* study, Garlic extract

DOI: https://dx.doi.org/10.22159/ijap.2025v17i1.52647 Journal homepage: https://innovareacademics.in/journals/index.php/ijap

INTRODUCTION

Nanotechnology is an interdisciplinary field focused on the manipulation and engineering of materials at the nanoscale, which generally spans dimensions between 1 and 100 nm. At this scale, materials display distinct properties and behaviors that are not observed at larger dimensions. The small size of nanoparticles (NPs) imparts distinctive properties, such as large surface area-to-volume ratios and quantum effects [1, 2]. These properties make NPs useful as drug delivery vehicles, particularly for cancer therapy. Owing to their diminutive size and expansive surface area, NPs carrying drugs exhibit heightened solubility, leading to improved bioavailability.

Novel Drug Delivery Systems (NDDS) are advanced techniques designed to enhance the delivery of drugs. These systems address the limitations of traditional drug delivery methods by improving bioavailability, enhancing solubility, controlling drug delivery, targeting specific sites within the body, and increasing patient compliance [3]. Additionally, NDDS enhances efficacy, reduces side effects, and increases convenience. They represent a significant evolution in the pharmaceutical industry, offering improved methods for drug administration that enhance therapeutic efficacy while minimizing side effects. Their continued development and implementation are crucial for advancing modern medicine [4].

Curcumin (CuR) is a natural polyphenol compound derived from the turmeric plant (*Curcuma longa*) with potential anticancer and anti-inflammatory properties. Additionally, CuR acts as a powerful antioxidant, scavenging free radicals and protecting cells from oxidative stress and DNA damage. Its ability to modulate cell cycle progression and induce apoptosis in cancer cells contributes to its anticancer effects. However, its clinical application is hampered by challenges related to low solubility, limited bioavailability, and rapid degradation [5, 6]. Hence, nanoparticle-based drug delivery systems have emerged as a solution to these challenges, facilitating enhanced stability, controlled release, and targeted delivery of therapeutic agents.

Garlic (*Allium sativum*-AS) has a long history of medicinal use, attributed to its bioactive compounds such as allicin, ajoene, and various sulfur-containing compounds. Renowned for its medicinal properties and rich bioactive content, AS offers a natural and sustainable avenue for creating nanoparticles (NPs). The decision to utilize AS stems from its abundance, biocompatibility, and the eco-friendly nature of green synthesis methods [7]. As a versatile source of bioactive compounds, AS not only serves as a stabilizing and reducing agent in NP synthesis but also provides antioxidant and therapeutic properties [8]. This dual role of AS in green synthesis aligns with the principles of sustainability, minimizing environmental impact and offering a promising pathway for the development of NPs with diverse applications, making AS an attractive candidate for NP formulation through a green synthesis approach [9].

The convergence of CuR and AS within the framework of NPs holds the promise of synergistic anticancer effects. Both CuR and AS compounds have individually demonstrated anticancer activities, and their combined potential, when encapsulated in NPs, is an uncharted territory that demands exploration [10]. This study aims to pioneer the green synthesis of CuR-loaded AS nanoparticles (C-AgNPs) and subsequently comprehensively characterize these NPs. Furthermore, the study seeks to evaluate the *in vitro* drug release and physicochemical properties of these NPs, specifically through Fourier-Transform Infrared Spectroscopy (FTIR), offering insights into their potential as effective therapeutic agents.

The green synthesis approach is a key aspect of this research, underscoring the commitment to environmentally sustainable practices. Traditional methods of nanoparticle (NP) synthesis often involve the use of harsh chemicals and energy-intensive processes, contributing to environmental degradation. In contrast, green

synthesis methods utilize natural resources and environmentally benign techniques, minimizing ecological impact and promoting sustainable technologies [11]. The incorporation of AS in this synthesis not only aligns with the green synthesis ethos but also highlights the inherent medicinal properties of AS compounds.

MATERIALS AND METHODS

The curcumin (CuR) used was obtained from Sisco Research laboratories Pvt. Ltd., (Maharashtra, India). Fresh garlic (*Allium sativum*-AS) cloves were purchased from the local market of Bandar Saujana Putra (Selangor, Malaysia). Silver nitrate ($AgNO_3$), ethanol and distilled water procured from Merck, Germany. All the experiments utilised double distilled water. Analytical-grade substances and components were used throughout.

Preparation of calibration curve

CuR concentration was estimated using the UV spectrophotometric technique. CuR was dissolved in ethanol, and the appropriate volume was added to prepare a stock solution of 1 mg/ml. Double-distilled water was used to further dilute this stock solution to obtain a concentration of 10 µg/ml. Aliquots of these solutions were placed into a quartz cell and subjected to a UV spectrophotometer (SECOMAM UviLine 9400, Selangor, Malaysia) to measure λmax in the 200–800 nm range, using double-distilled water as a blank. Plotting concentration against absorbance produced the standard calibration curve, with various CuR solution concentrations constructed in the range of 1–10 µg/ml [12].

Preparation of C-AgNPs

Preparation of AS extract

20 cloves of AS were used, with the outer skins manually removed. The AS cloves were then washed with sterile distilled water and allowed to air dry at room temperature for 1 h [13]. An aqueous fresh AS extract was prepared by grinding the cloves with 50 ml of double-distilled water using a Trio Blender, Chopper and Miller (Malaysia). The mixture was then filtered through Whatman filter paper (11 µm) to eliminate solid particles. The resulting filtrate was stored in the refrigerator at 4 °C for about 1 h while preparing the CuR and $AgNO_3$ solutions to maintain stability for subsequent use.

Green synthesis of silver nanoparticles (AgNPs)

For the synthesis of C-AgNPs, table 1 presents the appropriate quantities of CuR and $AgNO_3$. CuR was dissolved in 0.5 ml of ethanol and 0.5 ml of double-distilled water to form a CuR solution, while $AgNO_3$ was dissolved in 18 ml of distilled water to create an aqueous $AgNO_3$ solution. An appropriate quantity of aqueous AS extract was then added to the CuR solution and mixed well. Subsequently, 18 ml of the $AgNO_3$ solution was added to the mixture, which was continuously stirred (650 rpm) using a flat spin magnetic stirrer (Dragon Lab, Flatspin Magnetic Stirrer 8030184000, Selangor, Malaysia) and exposed to sunlight for the silver ion reduction process (35 °C under dry and hot conditions). After a few seconds (within 3 sec), the yellowish solution turned reddish-brown, indicating the formation of silver colloids [14]. The color intensity increased over time and plateaued after 15 min. Lastly, the sample was placed in a freeze dryer (ScanVac CoolSafe 110-4, Selangor, Malaysia) and allowed to freeze-dry for 36 h to obtain the final products. The procedure was repeated for the preparation of blank AgNPs; however, the formulation of AgNPs (B) was adjusted to use 100 mg of CuR and 50 mg of $AgNO_3$.

Drug assay and yield

Following a 2 ml ethanol dilution, pure CuR, AgNPs, and C-AgNPs equivalent to the weight of CuR were sonicated. Double-distilled water was used for further dilutions, and UV absorbance was recorded. A standard calibration curve at a wavelength of 423 nm was used to quantify the drug content, and the material balance was computed in relation to that content [15]. The following formula was used to calculate the yield percentage based on the initial amount.

$$\%\ Yield\ = \frac{Total\ weight\ of\ the\ C-AgNPs}{Total\ weight\ of\ the\ drug\ and\ additives}\ X\ 100 \quad \text{..... (1)}$$

Table 1: Various preparation of C-AGNPs

S. No.	Ingredients	Codes		
		C-AgNP1	C-AgNP2	C-AgNP3
1	CuR (mg)	50	100	75
2	$AgNO_3$ (mg)	100	50	50
3	AS extract (mL)	0.5	1	1.5

Drug loading (DL)

The freeze-dried C-AgNPs were dissolved in 0.5 ml of ethanol and an appropriate quantity of distilled water for dilution. The solution was then filtered through a 0.45 µm membrane filter, and the concentration was measured at 423 nm using a UV-Vis spectrophotometer [15]. The following equation was used to quantify the drug loading (DL) capacity from C-AgNPs.

$$Drug\ Loading = \frac{Amount\ of\ CuR\ in\ C-AgNPs}{Amount\ of\ C-AgNPs\ Obtained}\ x\ 100 \quad \text{..... (2)}$$

Percentage drug entrapment efficiency (%EE)

The CuR % encapsulation efficiency (%EE) in C-AgNPs was determined based on the supernatant collected during the nanoparticle formulation. The clear supernatant was obtained after centrifugation at 6000 rpm for 15 min and analyzed using UV-visible spectroscopy at 423 nm. The following equation (3) was used to calculate the drug %EE [16].

$$\%EE = \frac{Amount\ of\ CuR\ in\ C-AgNPs}{Total\ amount\ of\ CuR\ Used}\ x\ 100 \quad \text{..... (3)}$$

Fourier-transform infrared spectroscopy (FTIR) study

FTIR was used to confirm the formation of C-AgNPs and to determine the functional groups of CuR. Two milligrams of CuR, blank AgNPs, and C-AgNPs were scanned using an FTIR spectrometer (FTIR Perkin Elmer, Spectrum Two, Selangor, Malaysia) in the range of 4000–400 cm^{-1} with the settings of 20 scans and a resolution of 4 [16].

In vitro cur release

The dialysis bag method was used for the *in vitro* drug release investigation. A small quantity of PBS dissolving media was introduced to a cellulose dialysis bag (Molecular cutoff: 12,000 KDa) containing nanocrystals equivalent to 5 mg of the drug. The bag was sealed at both ends and placed in a beaker with 1x PBS and pH 6.4. At each time interval, 5 ml aliquots were removed and replaced with fresh dissolving media until 180 min. A UV spectrophotometer was used to test the samples at 423 nm [17].

Release kinetics

The dissolution release kinetics of the prepared C-AgNPs were calculated using first-and zero-order equations. Higuchi, Hixson-Crowell, Korsmeyer-Pappas, and release exponent (n) equation models were then used to further characterize the drug release mechanism [12]. To determine the pattern of release from the C-AgNPs, other parameters and the regression coefficient (R^2) were computed.

Statistical analysis

The data derived from three measurements taken in triplicate are reported as mean values and standard deviations. Statistical analysis was conducted using Student's t-test after performing a one-way

analysis of variance (ANOVA), with the analyses carried out using SPSS software.

RESULTS AND DISCUSSION

The λ_{max} of CuR was determined first by scanning solution of CuR in a UV spectrophotometer (fig. 1a) and the λ_{max} was found to be 423 nm as shown in fig. 1a and the calibration curve of CuR was plotted as shown as fig. 1b.

Drug content and yield

The amount of CuR present in the prepared C-AgNPs ranges from 92.23±8.41 to 96.11±7.82 % and the material loss concerning the CuR content was estimated to be 2.79± 0.81 to 4.86±0.93 % of the material (fig. 2). After obtaining the product, the higher material loss was observed with C-AgNPs3>C-AgNPs2>C-AgNPs1 due increased the concentration of AS extract according to the previous study [18].

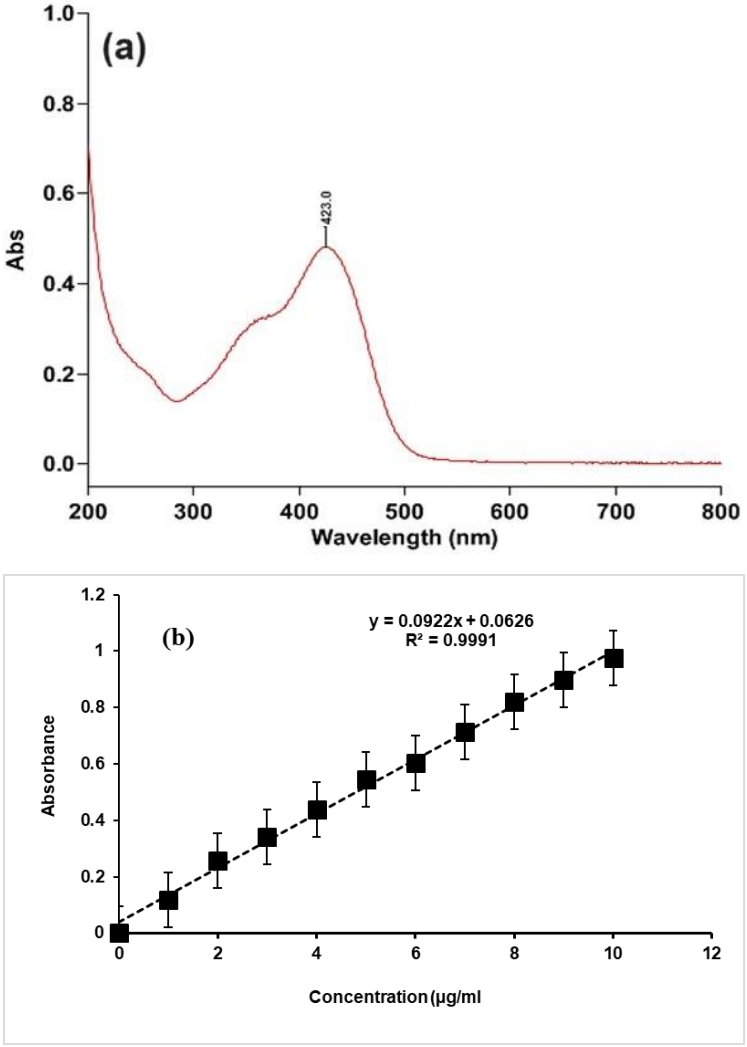

Fig. 1: (a) UV scan (at the concentration 5 µg/ml in the range of 200 to 800 nm) and (b) standard calibration curve of CuR, each value signifies mean±SD, n = 3

EE and DL

The C-AgNPs exhibited ideal drug loading (>60%). However, to increase drug loading, other factors such as reaction time, temperature, and the drug-to-Ag precursor ratio may need to be further considered and optimized. The percentages of encapsulation efficiency (EE) and drug loading (DL) of C-AgNPs varied from 58.56±4.18% to 74.24±5.87% and from 89.23±6.14% to 95.99±7.81% (fig. 2). Approximately 90% of the total output was due to the highest absorption of C-AgNPs, which occurred between 200 and 400 nm, with a peak observed at 423 nm (p>0.05). This measurement indicates that the EE was between 95% and 105% of CuR, which is the reference (label amount) range [19]. Due to its smaller size and maximum DL (95.99±7.81%) and EE (74.24±5.87%), CAgNP1 was chosen as the best formulation for this investigation. The lipophilic property of CuR (log P = 3.29) and the CuR: $AgNO_3$ ratio of C-AgNP1 were found to be 1:2. This suggests that incorporating a positively charged carrier, such as Ag^+, could enhance EE [20].

FTIR outcome

Fig. 3 displays the FT-IR spectra of AS extracts, pure CuR, $AgNO_3$, AgNPs, and CAgNPs that were used to prepare the nanoparticles (NPs). The wavenumbers for each spectrum and the characteristics of the functional bands observed are listed in table 2. The peak in the CuR spectrum at 3440.22 cm^{-1}, corresponding to –OH (alcohol) stretch vibrations, was present, suggesting the existence of a hydroxyl group. It was evident from the peaks at 1739.88 and 1631.29 cm^{-1} that the structure contained C=O (carbonyl) groups, indicative of the presence of a conjugated ketone group in the compound. According to an earlier investigation published by Mohamed *et al.* (2022), the C–H (alkane) stretch vibrations at 2931.01 and 2851.09 cm^{-1} and the C=C (aromatic) stretch vibrations at 1589.87 and 1510.23 cm^{-1} were also noticeable [21].

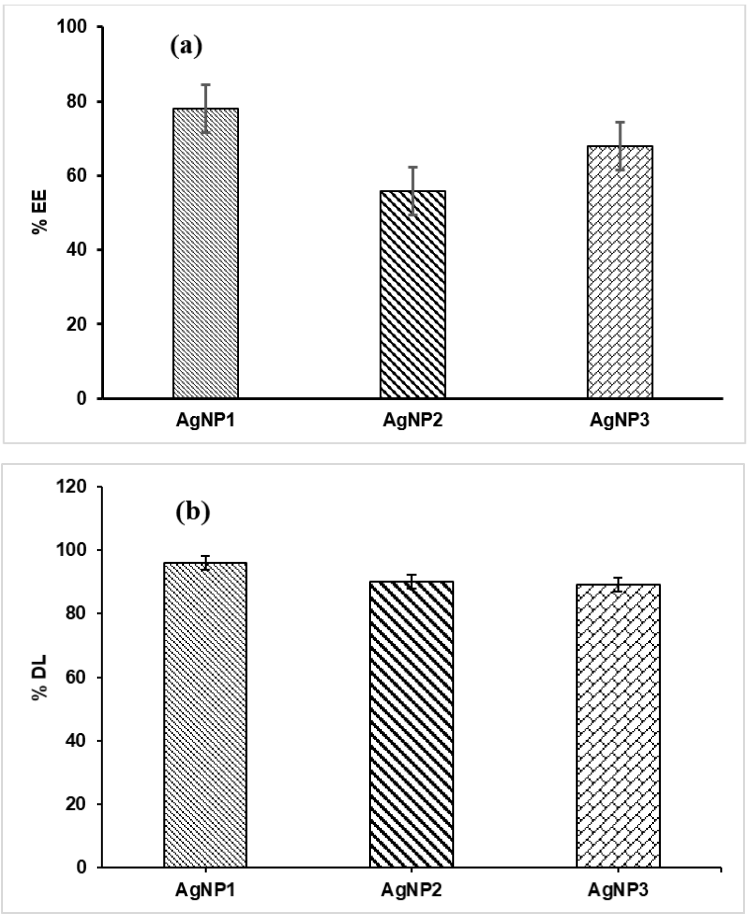

Fig. 2: (a) % EE and (b) % DL of prepared C-AgNPs. * Each value signifies mean±SD, n = 3

Table 2: FTIR spectrum and its wavelength of prepared C-AGNPs

Formulation	Absorption (cm^{-1})	Chemical groups	Compound class
C-AgNPs	3011.38	Weak O-H stretching	Alcohol
	1508.23	C-H bending	Alkane
	1225.14	Strong C-H stretching	Amine salt
	1205.44	Strong S=O stretching	Sulfonamide
	963.06, 807.90	C=C bending	Ester
AgNPs	3272.57	N-H stretching	Primary amine
	2936.72	C-H stretching	Alkane
	1507.09	C=N stretching	Imine/oxime
	1428.16	Strong S=O stretching	Sulfonamide
	1232.92, 1205.66	Strong C-O stretching	Ester
	963.33, 855.81	C=C bending	Ester
Pure CuR	3322.14, 3020.22	O-H stretching	Alcohol
	2931.01, 2851.09	C=C stretching	Aromatic
	1739.88, 1631.29	C=O stretching	Carbonyl
	1589.87, 1510.23	C-C stretching	Aromatic
$AgNO_3$	3419.23	O-H stretching	Alcohol
	1752.91, 1642.89	C=O stretching	Esters
	1308.07	C-H bending	Amine salt
	1044.23	S=O stretching	Sulfoxide
	829.89, 799.12	N-O bending	Nitro compound
AS Extract	3235.22	O-H stretching	Alcohol
	1741.12, 1625.29	C=O bending	Carbonyl
	1534.87	C-C stretching	Aromatic
	934.32	C=C bending	Ester

The FTIR spectrum of C-AgNPs (fig. 3) showed a peak at 3011.38 cm^{-1}, which indicated the presence of aromatic C–H stretching groups in CuR. The peaks at 1275.14 cm^{-1} and 1205.44 cm^{-1} corresponded to the stretching vibrations of the phenolic C–O bond in CuR. Additionally, the FTIR spectrum also showed a peak at 1508.23 cm^{-1}, indicating the presence of an aromatic ring in the AS extract, which acted as a reducing agent for the nanoparticles (NPs). CAgNPs with a higher concentration of CuR showed greater

intensity of peaks for the aromatic ring and phenolic hydroxyl groups [22].

The FTIR spectrum of $AgNO_3$ showed a peak at 800.69 cm^{-1}, reflecting the symmetric stretching of N–O bonds. $AgNO_3$ itself does not exhibit distinct peaks in the FTIR spectrum because it is a salt and lacks characteristic functional groups that produce strong IR absorptions. The FTIR spectrum of AS extract exhibited C–S stretching vibrations at 1098.67 cm^{-1}, indicating the presence of sulfur-containing compounds in AS, such as allicin. The peaks at 3331.14 cm^{-1} and 3020.22 cm^{-1}, corresponding to –OH (alcohol) stretch vibrations, suggest the existence of two hydroxyl groups. It was evident from the peaks at 1739.88 cm^{-1} and 1631.29 cm^{-1} that the structure contained C=O (carbonyl) groups.

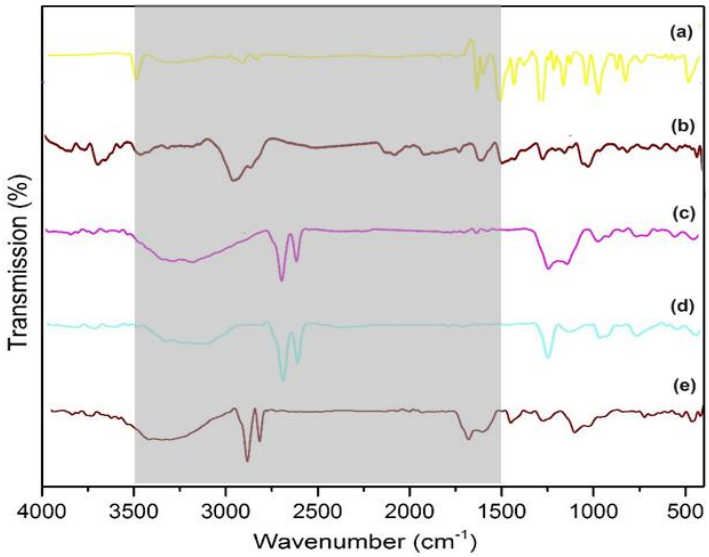

Fig. 3: FTIR spectrum of (a) Pure CuR, (b) $AgNO_3$, (c) AS extract, (d) AgNPs, and (e) C-AgNP1 were obserbed at 1500 – 3500 cm^{-1}

In vitro CuR release

Fig. 4 displays the cumulative CuR release profiles from C-AgNPs. As a control, pure CuR in 1X PBS was employed. For the *in vitro* release of CuR, a pH of 6.8 in PBS was selected, as it is similar to the physiological conditions of human tissues. The pH, which has been shown to be a crucial factor in many therapies, influences how the drug is released. Normal tissue has a different pH than disease-induced tissues and organs, depending on the pathological processes occurring in those tissues [23, 24]. Under the pH 6.8 condition, pure CuR release was sustained, and no early burst release was observed, suggesting a potentially advantageous use of the phytogenic C-AgNPs for topical and intravenous delivery.

The rate of CuR release was found to be half that of pure CuR in the pH 6.8 and internal gastrointestinal (GIT) environments. C-AgNPs demonstrated slower, more prolonged, and regulated drug release (sustained release). Maintaining the physiological pH of the body at 6.8 is beneficial, as the average amount of CuR released from C-AgNPs at that pH reduces the toxicity of CuR to normal tissue. Mohamed *et al.* (2022) also found that isoniazid (INH)-AgNCs exhibited a controlled and prolonged release (up to 180 min) of the drug; in pH 5.7 (weakly acidic) and pH 7.2 (neutral) conditions, the release rate was observed to be 3 to 4-fold lower than that of free INH [25].

Release kinetics

The Korsmeyer-peppas model (0.999±0.10) provided a better explanation for the *in vitro* release of CuR from C-AgNPs compared to the first-order (0.993±0.07) release kinetics, as displayed in table 3. The Korsmeyer-Peppas model is a mathematical equation used to describe drug release from polymeric matrices.

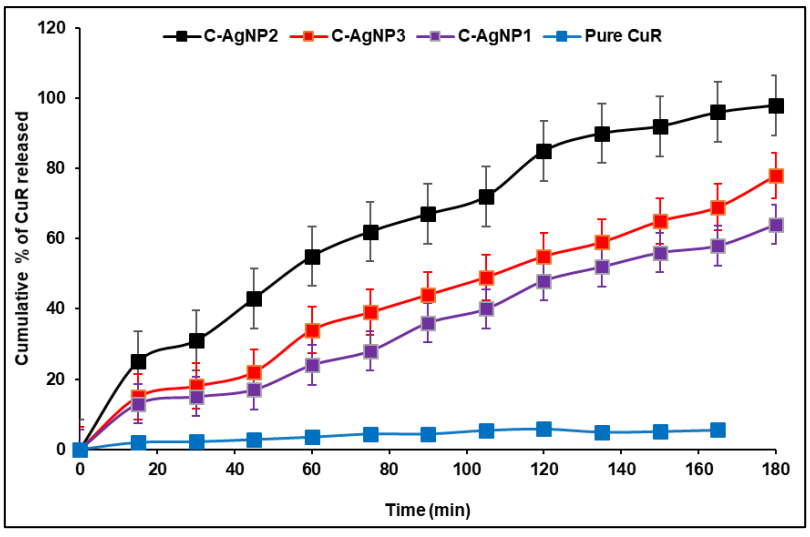

Fig. 4: *In vitro* CuR release from C-AgNPs prepared using AS as the reducing agent at 37 °C and pH 6.8. The control was 1X PBS containing pure CuR, *Each value signifies mean±SD, n = 3

Table 3: *In vitro* CuR release kinetics of free CuR and various C-AgNPs

Correlation coefficient (r^2)						Release exponent (n)
Codes	**Zero-order**	**First order**	**Higuchi**	**Hixon Crowell**	**Korsmeyer-peppas**	
Free CuR	0.887±0.05	0.982±0.09	0.872±0.03	0.962±0.02	0.870±0.08	0.421±0.04
C-AgNP1	0.989±0.06	0.993±0.07	0.966±0.08	0.712±0.09	0.999±0.10	0.773±0.02
C-AgNP2	0.883±0.14	0.989±0.08	0.892±0.12	0.954±0.18	0.997±0.05	0.672±0.09
C-AgNP3	0.891±0.09	0.979±0.08	0.971±0.05	0.941±0.21	0.980±0.06	0.681±0.09

*Each value signifies mean±SD, n=3.

The release mechanism was complex, involving both diffusion and other factors. The release rate is between Fickian and case II transport. This could be advantageous for controlled-release systems with a balance of rapid and sustained release fig. 5. Compared to free CuR, the release of CuR from C-AgNPs may be more effectively diffusion-controlled with a prolonged release. It relates the amount of drug released to time and a release exponent (n). This exponent provides insights into the mechanism of drug release. 0.5<n<1.0 (0.773±0.02), suggests anomalous diffusion. The drug release from C-AgNPs releases as a combination of Fickian diffusion and such as relaxation of the cross-linking complex with CuR with $AgNO_3$ chains [26].

By understanding the release exponent, researchers can tailor the properties of nanoparticles and polymeric matrices to achieve desired drug release profiles for various therapeutic applications [27].

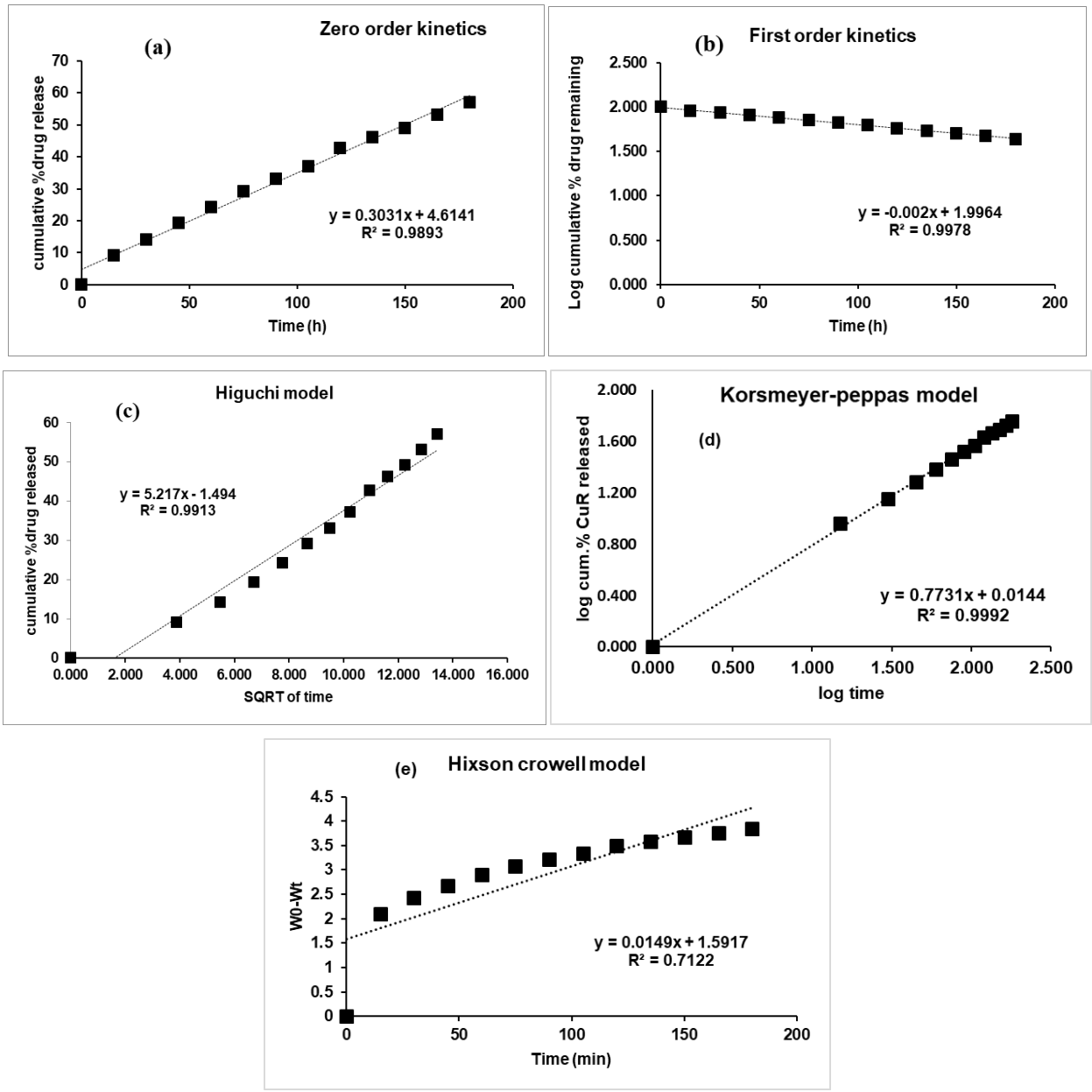

Fig. 5: Mechanism of CuR release kinetics of various models such as (a) zero-order, (b) first order, (c) Higuchi model, (d) Korsmeyer-Peppas model, and (e) Hixson-Crowell release from C-AGNP1

CONCLUSION

In summary, the ultra-fast synthesis of CuR-loaded silver nanoparticles has demonstrated significant advancements in the physicochemical properties critical for effective drug delivery. The study highlights the successful enhancement of drug loading capacity and entrapment efficiency, as evidenced by FTIR analysis and other characterization techniques. The *in vitro* drug release profiles indicate a controlled release mechanism, which can potentially improve therapeutic outcomes. These findings suggest that the developed silver nanoparticles not only enhance the bioavailability of CuR but also hold promise for applications in targeted drug delivery systems. Future studies should explore the *in vivo* efficacy and safety of these nanoparticles to further validate their potential in clinical settings. Additionally, future research should include particle size analysis to fully characterize the size distribution of the nanoparticles, which is crucial for optimizing their performance in drug delivery applications.

FUNDING

Nil

AUTHORS CONTRIBUTIONS

All authors contributed equally to that manuscript regarding design of experiments, experimental work, preparing and reviewing the manuscript before submission. All the authors contributed significantly to this manuscript, participated in reviewing/editing and approved the final draft for publication. Conceptualization (Jamal Moideen Muthu Mohamed); methodology (Jamal Moideen Muthu Mohamed and Chong Xue Li); software (Gamal Osman Elhassan); validation (Jamal Moideen Muthu Mohamed); formal analysis (Jamal Moideen Muthu Mohamed and Chong Xue Li, Riyaz Ahmed Khan); investigation (Gamal Osman Elhassan and Chong Xue Li); resources (Jamal Moideen Muthu Mohamed, Siham A. Abdoun and Gamal Osman Elhassan) data curation (Jamal Moideen Muthu Mohamed and Gamal Osman Elhassan); writing—original draft preparation (Manoj Goyal and Siham, Monika Bansal, A. Abdoun); review (Siham A. Abdoun and Riyaz Ahmed Khan); visualization (Jamal Moideen Muthu Mohamed and Riyaz Ahmed Khan); supervision (Jamal Moideen Muthu Mohamed); project administration (Manoj Goyal); funding acquisition (Gamal Osman Elhassan, Manoj Goyal and Monika Bansal).

CONFLICT OF INTERESTS

The authors have no conflicts of interest

REFERENCES

1. Khan I, Saeed K, Khan I. Nanoparticles: properties applications and toxicities. Arab J Chem. 2019;12(7):908-31. doi: 10.1016/j.arabjc.2017.05.011.
2. Azhar M, Mishra A. Review of nanoemulgel for treatment of fungal infections. Int J Pharm Pharm Sci. 2024;16(9):8-17. doi: 10.22159/ijpps.2024v16i9.51528.
3. Ezike TC, Okpala US, Onoja UL, Nwike CP, Ezeako EC, Okpara OJ. Advances in drug delivery systems challenges and future directions. Heliyon. 2023;9(6):e17488. doi: 10.1016/j.heliyon.2023.e17488, PMID 37416680.
4. Patra JK, Das G, Fraceto LF, Campos EV, Rodriguez Torres MD, Acosta Torres LS. Nano-based drug delivery systems: recent developments and future prospects. J Nanobiotechnology. 2018;16(1):71. doi: 10.1186/s12951-018-0392-8, PMID 30231877.
5. Sharifi Rad J, Rayess YE, Rizk AA, Sadaka C, Zgheib R, Zam W. Turmeric and its major compound curcumin on health: bioactive effects and safety profiles for food pharmaceutical biotechnological and medicinal applications. Front Pharmacol. 2020;11:01021. doi: 10.3389/fphar.2020.01021, PMID 33041781.
6. Adarsa S, Babu AS, Sunil S, Jomine Jose J. Axillary lymph node metastasis in sonologically node-negative breast carcinoma. Asian J Pharm Clin Res. 2024;17(10):26-9. doi: 10.22159/ajpcr.2024v17i10.52192.
7. Shang A, Cao SY, XU XY, Gan RY, Tang GY, Corke H. Bioactive compounds and biological functions of garlic (*Allium sativum* L.). Foods. 2019;8(7):246. doi: 10.3390/foods8070246, PMID 31284512.
8. Melguizo Rodriguez L, Garcia Recio E, Ruiz C, DE Luna Bertos E, Illescas Montes R, Costela Ruiz VJ. Biological properties and therapeutic applications of garlic and its components. Food Funct. 2022;13(5):2415-26. doi: 10.1039/d1fo03180e, PMID 35174827.
9. Elfiyani R, Radjab NS, Wijaya AN. Garlic extract phytosome: preparation and physical stability. Int J App Pharm. 2024;16(1):118-25. doi: 10.22159/ijap.2024.v16s1.27.
10. Pandey P, Khan F, Alshammari N, Saeed A, Aqil F, Saeed M. Updates on the anticancer potential of garlic organosulfur compounds and their nanoformulations: plant therapeutics in cancer management. Front Pharmacol. 2023 Mar 20;14:1154034. doi: 10.3389/fphar.2023.1154034, PMID 37021043.
11. Bhardwaj B, Singh P, Kumar A, Kumar S, Budhwar V. Eco-friendly greener synthesis of nanoparticles. Adv Pharm Bull. 2020;10(4):566-76. doi: 10.34172/apb.2020.067, PMID 33072534.
12. Mohamed JM, Alqahtani A, Ahmad F, Krishnaraju V, Kalpana K. Stoichiometrically governed curcumin solid dispersion and its cytotoxic evaluation on colorectal adenocarcinoma cells. Drug Des Devel Ther. 2020 Nov 2;14:4639-58. doi: 10.2147/DDDT.S273322, PMID 33173275.
13. LI G, MA X, Deng L, Zhao X, Wei Y, Gao Z. Fresh garlic extract enhances the antimicrobial activities of antibiotics on resistant strains *in vitro.* Jundishapur J Microbiol. 2015;8(5):e14814. doi: 10.5812/jjm.14814, PMID 26060559.
14. Asif M, Yasmin R, Asif R, Ambreen A, Mustafa M, Umbreen S. Green synthesis of silver nanoparticles (AgNPs) structural characterization and their antibacterial potential. Dose Response. 2022 Apr 30;20(2):15593258221088709. doi: 10.1177/15593258221088709, PMID 35592270.
15. Muthu J, Ahmad F, Kishore N, Al Subaie AM. Soluble 1: 1 stoichiometry curcumin binary complex for potential apoptosis in human colorectal adenocarcinoma cells (SW480 and CACO-2 cells). Res J Pharm Technol. 2021;14(1):129-35. doi: 10.5958/0974-360X.2021.00023.8.
16. Mohamed JM, Alqahtani A, Kumar TV, Fatease AA, Alqahtani T, Krishnaraju V. Superfast synthesis of stabilized silver nanoparticles using aqueous Allium sativum (garlic) extract and isoniazid hydrazide conjugates: molecular docking and *in vitro* characterizations. Molecules. 2021;27(1):110. doi: 10.3390/molecules27010110, PMID 35011342.
17. Alqahtani A, Raut B, Khan S, Mohamed JM, Fatease AA, Alqahtani T. The unique carboxymethyl fenugreek gum gel loaded itraconazole self-emulsifying nanovesicles for topical onychomycosis treatment. Polymers (Basel). 2022;14(2). doi: 10.3390/polym14020325, PMID 35054731.
18. Mohamed JM, Ahmad F, Alqahtani A, Lqahtani T, Raju VK, Anusuya M. Studies on preparation and evaluation of soluble 1:1 stoichiometric curcumin complex for colorectal cancer treatment. Trends Sci. 2021;18(24):1403. doi: 10.48048/tis.2021.1403.
19. Bodke V, Kumbhar P, Belwalkar S, Mali AS, Waghmare K. Design and development of nanoemulsion of smilax china for anti-psoriasis activity. Int J Pharm Pharm Sci. 2024;16(5):54-66. doi: 10.22159/ijpps.2024v16i5.50327.
20. Mohamed JM, Alqahtani A, Khan BA, Al Fatease A, Alqahtani T, Venkatesan K. Preparation of soluble complex of curcumin for the potential antagonistic effects on human colorectal adenocarcinoma cells. Pharmaceuticals (Basel). 2021;14(9):939. doi: 10.3390/ph14090939, PMID 34577638.
21. Mohamed JM, Alqahtani A, Ahmad F, Krishnaraju V, Kalpana K. Pectin co-functionalized dual layered solid lipid nanoparticle made by soluble curcumin for the targeted potential treatment of colorectal cancer. Carbohydr Polym. 2021;252:117180. doi: 10.1016/j.carbpol.2020.117180, PMID 33183627.
22. Gautham U, Patil A, Hemanth G. Formulation and evaluation of nanoparticle drug delivery system for treatment of hypertension. Int J App Pharm. 2023;15(6):90-7. doi: 10.22159/ijap.2023v15i6.48971.
23. Almalla A, Elomaa L, Bechtella L, Daneshgar A, Yavvari P, Mahfouz Z. Papain-based solubilization of decellularized extracellular

matrix for the preparation of bioactive thermosensitive pregels. Biomacromolecules. 2023;24(12):5620-37. doi: 10.1021/acs.biomac.3c00602, PMID 38009757.

24. Mohamed JM, Alqahtani A, Kumar TV, Fatease AA, Alqahtani T, Krishnaraju V. Superfast synthesis of stabilized silver nanoparticles using aqueous allium sativum (garlic) extract and isoniazid hydrazide conjugates: molecular docking and *in vitro* characterizations. Molecules. 2021;27(1):110. doi: 10.3390/molecules27010110, PMID 35011342.
25. FU Y, Kao WJ. Drug release kinetics and transport mechanisms of non-degradable and degradable polymeric delivery systems. Expert Opin Drug Deliv. 2010;7(4):429-44. doi: 10.1517/17425241003602259, PMID 20331353.
26. Bayer IS. Controlled drug release from nanoengineered polysaccharides. Pharmaceutics. 2023;15(5):1364. doi: 10.3390/pharmaceutics15051364, PMID 37242606.
27. M Ewedah T, El nabarawi M, H Teaima M, Elhabal SF, R Shoueir K, Hamdy AM. Development and optimization of the wound healing electrospun polyurethane/collagen/phytoceramides nanofibers using the box behnken experimental design) quality by design). Int J App Pharm. 2024;16(5):99-100. doi: 10.22159/ijap.2024v16i5.51510.